DOI: 10.1002/ejic.201000443

Synthesis, Structures and Electrochemistry of New Carbonylnickel Octacarbide Clusters: The Distorting Action of Carbide Atoms in the Growth of Ni Cages and the First Example of the Inclusion of a Carbon Atom within a (Distorted) Ni Octahedral Cage

Alessandro Bernardi,[a] Cristina Femoni,[a] Maria Carmela Iapalucci,[a] Giuliano Longoni,[a] Stefano Zacchini,*[a] Serena Fedi,[b] and Piero Zanello[b]

Keywords: Cluster compounds / Carbonyl ligands / Electrochemistry / Nickel / Carbides

The reaction of $[Ni_{10}C_2(CO)_{15}]^{2-}$ in thf with a large excess of $CdCl_2{\cdot}2.5H_2O$ (8–15 equiv.) resulted in the formation of the new carbonyl octacarbide clusters $[H_{5-n}Ni_{36}C_8(CO)_{36}(Cd_2Cl_3)]^{n-}$ (n = 3–5), which undergo partial CO replacement to give $[Ni_{36-y}C_8(CO)_{34-y}(MeCN)_3(Cd_2Cl_3)]^{3-}$ (y = 0–2) after a prolonged time in MeCN. Treatment of the former with an excess of NaOH afforded the larger $[H_{7-n}Ni_{42+y}C_8(CO)_{44+y}(CdCl)]^{n-}$ (n = 6, 7; y = 0, 1) octacarbides. Their structures (as well as those of the analogous Br-containing clusters) have been fully elucidated by single-crystal X-ray analysis of their $[Me_4N]_5[Ni_{36}C_8(CO)_{36}(Cd_2Cl_3)]{\cdot}(7–2y)MeCN{\cdot}yC_6H_{14}$ (y = 0.40), $[Me_4N]_3[Ni_{36-y}C_8(CO)_{34-y}(MeCN)_3(Cd_2Cl_3)]{\cdot}5MeCN$ (y = 0.61), $[Me_4N]_7[Ni_{42+y}C_8(CO)_{44+y}(CdCl)]{\cdot}(5–y)MeCN$ (y = 0.19) and $[Me_4N]_6[HNi_{42+y}C_8(CO)_{44+y}(CdBr)]{\cdot}(6–y)MeCN$ (y = 0.19) salts, which feature highly distorted metal cages (due to the inclusion of several carbide atoms), and the presence of partially vacant capping Ni(CO) fragments. This aspect, together with the fact that all these species undergo several protonation–deprotonation equilibria in solution as well as reversible redox processes under electrochemical control, indicates that a detailed description of molecular species containing a few dozen metal atoms might be sometimes rather troublesome and non-trivial. A complete elucidation of these systems can be achieved only by combining structural, chemical, spectroscopic, electrochemical and spectroelectrochemical studies.

Introduction

Large molecular metal clusters stabilised by miscellaneous ligands, among which are metal carbonyl clusters (MCCs), are molecules or molecular ions perfectly defined in size, composition and structural detail, which trespass by size the field of nanomaterials at the lowest limit, and their chemistry and physical behaviour overlap with that of ligand-stabilised metal colloids.[1–3]

The structures of high-nuclearity MCCs are a result of the subtle balances between M–M and M–CO interactions, and – in the case of di- and heterometallic MCCs – these are further complicated by the presence of M–M′ and M–E interactions. Generally speaking, very large homo- and dimetallic MCCs usually adopt close-packed structures in which a chunk of ccp or hcp metal lattice is surrounded by a shell of CO ligands.[4–6]

The deviation from close-packing of the metal core in large MCCs is almost systematic in the presence of interstitial or peripheral main-group elements. In particular, high-nuclearity carbide MCCs display rather complex structures.[7] The number as well as the relative size of the interstitial carbide atoms and the metals composing the cluster are of paramount importance; with the notable exception of $[Ru_{10}C(CO)_{24}]^{2-}$, $[Os_{10}C(CO)_{24}]^{2-}$ and $[Os_{11}C(CO)_{27}]^{2-}$,[8,9] the metal cage very usually displays large deformations to generate cavities of suitable dimensions to allocate the heteroatoms. This is very well represented by the chemistry of Ni carbide MCCs.[10–15] Species containing from one up to eight C atoms are known, and their Ni/C ratios range from 10 to 2.75. Species with higher Ni/C ratios usually present isolated C atoms (one, four or six for the species reported up to now) within trigonal-prismatic (simple or monocapped) or square-antiprismatic cages. Conversely, as the Ni/C ratio decreases, strong C–C bonds are formed within the cluster, as shown by the evolution of C_2 and C_3 hydrocarbons upon hydrolysis.[16] So far, Ni acetylide MCCs containing one, two or four C_2 units are known.[14,15,17] This must be contrasted by the fact that carbon is very poorly soluble in bulk Ni, and only the metastable Ni_3C phase is known,[18] which possesses a ccp structure.

[a] Dipartimento di Chimica Fisica ed Inorganica, Università di Bologna, Viale Risorgimento 4, 40136 Bologna, Italy
Fax: +39-051-2093690
E-mail: zac@ms.fci.unibo.it
[b] Dipartimento di Chimica, Università di Siena, via De Gasperi 2, 53100 Siena, Italy

Supporting information for this article is available on the WWW under http://dx.doi.org/10.1002/ejic.201000443.

We herein report the first examples of (carbonyl)Ni octacarbide clusters {i.e., $[H_{5-n}Ni_{36}C_8(CO)_{36}(Cd_2Cl_3)]^{n-}$ (n = 3–5), $[Ni_{36-y}C_8(CO)_{34-y}(MeCN)_3(Cd_2Cl_3)]^{3-}$ (y = 0–2) and $[H_{7-n}Ni_{42+y}C_8(CO)_{44+y}(CdX)]^{n-}$ (n = 6,7; X = Cl, Br, y = 0, 1)}, which – in contrast to the previously reported tetraacetylide species, $[Ni_{22}(C_2)_4(CO)_{28}Cl]^{3-}$,[15] $[H_{4-n}Ni_{22}(C_2)_4(CO)_{28}(CdCl)_2]^{n-}$ (n = 2–4)[14] and $[HNi_{25}(C_2)_4(CO)_{32}]^{3-}$[15] – only display isolated interstitial C atoms. Electrochemical and spectroelectrochemical investigations confirm the multivalent nature of these large clusters.

Results and Discussion

Synthesis, Characterisation and Reactivity of $[H_{5-n}Ni_{36}C_8(CO)_{36}(Cd_2X_3)]^{n-}$ (n = 3–5; X = Cl, Br, I)

The reaction of $[Ni_{10}C_2(CO)_{15}]^{2-}$ in thf with a large excess of $CdCl_2{\cdot}2.5H_2O$ (8–15 equiv.) results in the formation of the new carbonyl octacarbide clusters $[H_{5-n}Ni_{36}C_8(CO)_{36}(Cd_2Cl_3)]^{n-}$ (n = 3–5) in good yields. These species are polyhydrides that display protonation–deprotonation equilibria depending on the basicity of the solvent, as previously found for other high-nuclearity MCCs.[12–15] In particular, the species directly obtained by performing the reaction in thf is the dihydride trianion $[H_2Ni_{36}C_8(CO)_{36}(Cd_2Cl_3)]^{3-}$.

It is very important to operate in thf and with a very large excess of Cd^{II} salts, otherwise the reaction has a different outcome, as previously reported. In particular, as shown in Scheme 1, by decreasing the amount of $CdCl_2{\cdot}2.5H_2O$ and independently of the solvent, significant amounts of the known tetracarbides $[H_{6-n}Ni_{30}C_4(CO)_{34}(CdCl)_2]^{n-}$ (n = 3–6)[12] are formed. Conversely, by operating in acetone with a large excess of $CdCl_2{\cdot}2.5H_2O$ (8–15 equiv.) the tetraacetylide $[H_{4-n}Ni_{22}(C_2)_4(CO)_{28}(CdCl)_2]^{n-}$ (n = 2–4)[14] is obtained. Thus, the reaction between $[Ni_{10}C_2(CO)_{15}]^{2-}$ and $CdCl_2{\cdot}2.5H_2O$ seems to be very sensitive to the experimental conditions, and it can result in three different products, depending on the stoichiometry and the reaction medium.

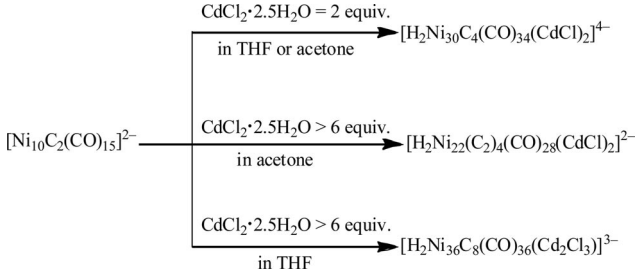

Scheme 1.

As shown in Scheme 1, the highest $CdCl_2{\cdot}2.5H_2O/[Ni_{10}C_2(CO)_{15}]^{2-}$ ratios lead to the prevailing formation of $[H_{5-n}Ni_{36}C_8(CO)_{36}(Cd_2Cl_3)]^{n-}$ (n = 3–5) in thf and $[H_{4-n}Ni_{22}(C_2)_4(CO)_{28}(CdCl)_2]^{n-}$ (n = 2–4) in acetone. However, in both cases smaller amounts of $[H_2Ni_{30}C_4(CO)_{34}(CdCl)_2]^{4-}$ are always found. The latter is the most abundant product in both reaction solvents only when the $CdCl_2{\cdot}2.5H_2O/[Ni_{10}C_2(CO)_{15}]^{2-}$ ratio is kept low (ca. 2). In any case, only mixtures of $[H_2Ni_{30}C_4(CO)_{34}(CdCl)_2]^{4-}$ with $[H_2Ni_{36}C_8(CO)_{36}(Cd_2Cl_3)]^{3-}$ (reaction in thf) or $[H_{4-n}Ni_{22}(C_2)_4(CO)_{28}(CdCl)_2]^{n-}$ (n = 2–4; reaction in acetone) are obtained as a function of the reaction solvent. Separation of the two different mixtures can be achieved owing to differential solubilities. In particular, $[H_2Ni_{36}C_8(CO)_{36}(Cd_2Cl_3)]^{3-}$ can be conveniently extracted in thf, whereas $[H_2Ni_{30}C_4(CO)_{34}(CdCl)_2]^{4-}$ is soluble in acetone.

The dihydride trianion $[H_2Ni_{36}C_8(CO)_{36}(Cd_2Cl_3)]^{3-}$, dissolved in thf, displays ν_{CO} bands at 2030 (s) and 1854 (m) cm^{-1}, whereas the carbonyl stretching bands are shifted towards lower frequencies in MeCN, that is, 2014 (s) and 1856 (br.) cm^{-1}; a further shift to even lower frequencies is observed after dissolution in dmf, that is, 2004 (s) and 1846 (m) cm^{-1}. These changes in ν_{CO} cannot be explained only on the basis of solvation effects, but they are in better agreement with protonation–deprotonation equilibria depending on the basicity of the solvent, which results in a net cluster charge change (Scheme 2).

Therefore, the species present in thf is the dihydride trianion $[H_2Ni_{36}C_8(CO)_{36}(Cd_2Cl_3)]^{3-}$, which is deprotonated to the monohydride tetraanion $[HNi_{36}C_8(CO)_{36}(Cd_2Cl_3)]^{4-}$ in MeCN and, finally, to the pentaanion $[Ni_{36}C_8(CO)_{36}(Cd_2Cl_3)]^{5-}$ after dissolution in the more basic dmf. The same changes in the IR spectra reported in Scheme 2 can be obtained by addition of acids or bases to solutions containing the different $[H_{5-n}Ni_{36}C_8(CO)_{36}(Cd_2Cl_3)]^{n-}$ (n = 3–5) anions. Note that the addition of chemical oxidants or reducing agents gives rise to decomposition, whereas under electrochemical control the completely deprotonated species affords stable reduced species (see the section Electrochemical and Spectroelectrochemical Studies). This further confirms that the different anions are related by protonation–deprotonantion reactions (and therefore they possess a polyhydride nature) and not by redox processes.

Crystals of the pentaanion $[Ni_{36}C_8(CO)_{36}(Cd_2Cl_3)]^{5-}$ suitable for X-ray analysis in the form of the $[Me_4N]_5[Ni_{36}C_8(CO)_{36}(Cd_2Cl_3)]{\cdot}(7–2y)MeCN{\cdot}yC_6H_{14}$ (y = 0.40) salt were obtained by slow diffusion of *n*-hexane and diisopropyl ether into an MeCN solution of the tetraanion, which suggests that crystallisation is accompanied by complete deprotonation. Dissolution of the crystals in MeCN gives back $[HNi_{36}C_8(CO)_{36}(Cd_2Cl_3)]^{4-}$ as the main species present in solution, as clearly indicated by IR spectroscopy.

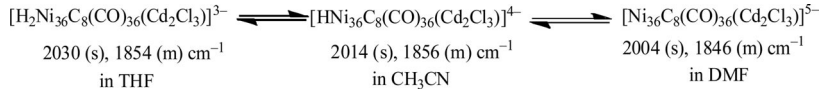

Scheme 2.

Similar behaviour has previously been reported for other MCCs, and among these other dimetallic Ni–Cd polycarbides have been demonstrated to possess a polyhydride nature, that is, $[H_{4-n}Ni_{22}(C_2)_4(CO)_{28}(CdX)_2]^{n-}$ (n = 2–4; X = Cl, Br),[14] $[H_{6-n}Ni_{30}C_4(CO)_{34}(CdX)_2]^{n-}$ (n = 3–6; X = Cl, Br, I)[12] and $[H_{7-n}Ni_{32}C_4(CO)_{36}(CdX)]^{n-}$ (n = 5–7; X = Cl, Br, I).[13] Only in the case of $[H_{4-n}Ni_{22}(C_2)_4(CO)_{28}(CdBr)_2]^{n-}$ (n = 2–4) was direct ^{1}H NMR proof for the presence and the number of the hydride atoms obtained, whereas in all other cases only indirect (chemical and electrochemical) evidence of the polyhydride nature of the clusters was obtained. Moreover, ^{1}H NMR studies on $[H_{4-n}Ni_{22}(C_2)_4(CO)_{28}(CdBr)_2]^{n-}$ (n = 2–4) in different solvents and at variable temperature indicated the presence of dynamic processes as well as a considerable line-broadening at all temperatures, which is not yet well understood. Nonetheless, this behaviour suggests that the ^{1}H NMR resonances for hydride atoms in high-nuclearity Ni MCCs might become increasingly broad as the nuclearity increases, until above a certain nuclearity they completely disappear in the baseline. In keeping with this trend, it has not been possible to prove the presence of hydride ligands in $[H_{5-n}Ni_{36}C_8(CO)_{36}(Cd_2Cl_3)]^{n-}$ (n = 3–5) by ^{1}H NMR spectroscopy.

Indirect proof of the total number of hydride ligands present in $[H_{5-n}Ni_{36}C_8(CO)_{36}(Cd_2Cl_3)]^{n-}$ (n = 3–5) is given by the observation that the reaction in MeCN of the tetraanion $[HNi_{36}C_8(CO)_{36}(Cd_2Cl_3)]^{4-}$ with an excess of NaOH first results in the formation of the pentaanion $[Ni_{36}C_8(CO)_{36}(Cd_2Cl_3)]^{5-}$ (as confirmed by IR spectroscopy) and then in the complete rearrangement of the cluster to give $[H_{7-n}Ni_{42+y}C_8(CO)_{44+y}(CdCl)]^{n-}$ (n = 6, 7; y = 0, 1; see the next section). This reaction is reminiscent of the transformation of $[H_{6-n}Ni_{30}C_4(CO)_{34}(CdX)_2]^{n-}$ (n = 3–6; X = Cl, Br, I) into $[H_{7-n}Ni_{32}C_4(CO)_{36}(CdX)]^{n-}$ (n = 5–7; X = Cl, Br, I) by nucleophilic attack on Cd^{II} by OH^- or X^- ions.[13]

Detailed studies on the behaviour in solution of $[H_{5-n}Ni_{36}C_8(CO)_{36}(Cd_2Cl_3)]^{n-}$ (n = 3–5) are complicated because ligand-substitution reactions may occur. In particular, the CO ligands are partially substituted by MeCN molecules after leaving the tetraanion $[HNi_{36}C_8(CO)_{36}(Cd_2Cl_3)]^{4-}$ in MeCN for a longer time (ca. 1 week), yielding species such as $[Ni_{36}C_8(CO)_{34}(MeCN)_3(Cd_2Cl_3)]^{3-}$. Crystals suitable for X-ray analysis of the trianion $[Ni_{36}C_8(CO)_{34}(MeCN)_3(Cd_2Cl_3)]^{3-}$, in the form of the salt $[Me_4N]_3[Ni_{36-y}C_8(CO)_{34-y}(MeCN)_3(Cd_2Cl_3)]\cdot 5MeCN$ (y = 0.61), were obtained by slow diffusion of *n*-hexane and diisopropyl ether in an MeCN solution of the cluster. The fractional indexes are due to the fact that two Ni(CO) groups in the cluster structure have fractional occupation factors. The substitution reaction is not complete and, therefore, the $[Ni_{36}C_8(CO)_{34}(MeCN)_3(Cd_2Cl_3)]^{3-}$ anion is always obtained as a mixture with the parent $[H_{5-n}Ni_{36}C_8(CO)_{36}(Cd_2Cl_3)]^{n-}$ (n = 3–5).

In a similar way, the reactions of $[Ni_{10}C_2(CO)_{15}]^{2-}$ in thf with a large excess of other Cd^{II} salts, such as $CdBr_2\cdot xH_2O$ and $CdI_2\cdot xH_2O$, result in the formation of analogous species $[H_{5-n}Ni_{36}C_8(CO)_{36}(Cd_2X_3)]^{n-}$ (n = 3–5; X = Br, I), even if in different yields. In fact, the bromine-containing species can be obtained as satisfactorily as the chlorine analogues, and their reactivities have consequently been studied (see the next section). Conversely, the iodine-containing species have always been obtained in low yields and their formation confirmed only spectroscopically.

Synthesis and Characterisation of $[H_{7-n}Ni_{42+y}C_8(CO)_{44+y}(CdX)]^{n-}$ (n = 6, 7; X = Cl, Br; y = 0, 1)

As described in the previous section, the reactions of the pentaanions $[Ni_{36}C_8(CO)_{36}(Cd_2X_3)]^{5-}$ (X = Cl, Br) with an excess of solid NaOH in MeCN result in the formation of the new octacarbides $[H_{7-n}Ni_{42+y}C_8(CO)_{44+y}(CdX)]^{n-}$ (n = 6, 7; X = Cl, Br; y = 0, 1) As described below, they are actually mixtures of two species, that is, $[H_{7-n}Ni_{42}C_8(CO)_{44}(CdX)]^{n-}$ (major) and $[H_{7-n}Ni_{43}C_8(CO)_{45}(CdX)]^{n-}$ (minor; n = 6, 7; X = Cl, Br). These anions can be obtained quite pure from other species after removal of the solvent under reduced pressure, washing of the residue with water and extraction in MeCN. Conversely, because of their very similar properties, these two species are always obtained as a mixture.

Their MeCN solutions display similar IR spectra for both the chlorine and bromine derivatives, that is, ν_{CO} bands at 2009 (s) and 1851 (m) cm^{-1} and at 2004 (s) and 1847 (m) cm^{-1}, respectively, and can be attributed to the hexaanionic clusters $[HNi_{42+y}C_8(CO)_{44+y}(CdX)]^{6-}$ (X = Cl, Br; y = 0, 1). Crystals suitable for X-ray analyses of the heptaanion $[Ni_{42+y}C_8(CO)_{44+y}(CdCl)]^{7-}$ and the hexaanion $[HNi_{42+y}C_8(CO)_{44+y}(CdBr)]^{6-}$ in the form of their salts $[Me_4N]_7[Ni_{42+y}C_8(CO)_{44+y}(CdCl)]\cdot(5-y)MeCN$ (y = 0.19) and $[Me_4N]_6[HNi_{42+y}C_8(CO)_{44+y}(CdBr)]\cdot(6-y)MeCN$ (y = 0.19), respectively, were obtained by slow diffusion of *n*-hexane and diisopropyl ether in their MeCN solutions. The formation of the heptaanion in the former case might be attributed to a protonation–deprotonation equilibrium present in solution and involving $[HNi_{42+y}C_8(CO)_{44+y}(CdCl)]^{6-}$ and $[Ni_{42+y}C_8(CO)_{44+y}(CdCl)]^{7-}$. The hexaanion is the prevailing species present in solution (as shown by IR), whereas the equilibrium is shifted towards the heptaanion during crystallisation. It must be remarked that this shift has been observed for the chlorine derivative but not for the bromine one, which indicates that accidental conditions occurring during crystallisation might favour the crystallisation of either the hepta- or the hexaanion. Note that the same IR spectra reported above are obtained by dissolving the $[Me_4N]_7[Ni_{42+y}C_8(CO)_{44+y}(CdCl)]\cdot(5-y)MeCN$ (y = 0.19) and $[Me_4N]_6[HNi_{42+y}C_8(CO)_{44+y}(CdBr)]\cdot(6-y)MeCN$ (y = 0.19) crystals in MeCN or dmf, which indicates that in all cases the heptaanion is protonated back to the hexaanion in solution, probably by traces of water contained in the solvents. Nonetheless, a considerable shift towards lower frequencies is observed in the solid state for the heptaanion in $[Me_4N]_7[Ni_{42+y}C_8(CO)_{44+y}(CdCl)]\cdot(5-y)MeCN$ (y = 0.19) [$\tilde{\nu}_{CO}$ = 2000 (w), 1975 (vs), 1833 (ms) and 1779 (m) cm^{-1} in a Nujol mull].

Crystal Structure of $[Me_4N]_5[Ni_{36}C_8(CO)_{36}(Cd_2Cl_3)]\cdot(7–2y)MeCN\cdot yC_6H_{14}$ (y = 0.40)

The crystal structure of the pentaanion $[Ni_{36}C_8(CO)_{36}(Cd_2Cl_3)]^{5-}$ was determined by single-crystal X-ray diffraction analysis of the $[Me_4N]_5[Ni_{36}C_8(CO)_{36}(Cd_2Cl_3)]\cdot(7–2y)MeCN\cdot yC_6H_{14}$ (y = 0.40) salt (Figure 1 and Table 1). The anion can be viewed as being composed of an $[Ni_{36}C_8(CO)_{36}]^{6-}$ carbonylmetal carbide frame to which a $[Cd_2Cl_3]^+$ fragment is coordinated, and overall it possesses an idealised C_{2v} symmetry.

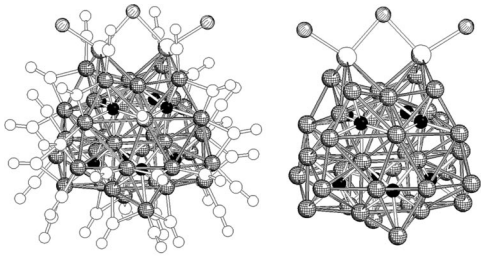

Figure 1. Molecular structure of (a) $[Ni_{36}C_8(CO)_{36}(Cd_2Cl_3)]^{5-}$ and (b) its metal carbide cage. Ni: two-direction fully hatched spheres; Cd: semi-hatched spheres; Cl: one-direction fully hatched spheres; interstitial carbide atoms: black spheres.

The cluster contains eight interstitial carbide atoms of which four are in strongly distorted octahedral cavities, two in trigonal-prismatic cavities and two in monocapped trigonal-prismatic cavities. Therefore, $[Ni_{36}C_8(CO)_{36}(Cd_2Cl_3)]^{5-}$ is the first carbonylnickel cluster in which interstitial carbon atoms are present in an octahedral environment, even though heavily distorted. The large deformation of the octahedral cavities in the present case is, probably, the result of the fact that the carbon atom is too large to fit in a compact nondistorted Ni cage. At the same time, these deformations are made possible by the fact that the metal cages in carbonyl clusters are relatively soft and overall protected and stabilised by the CO shell.

Crystal Structure of $[Me_4N]_3[Ni_{36-y}C_8(CO)_{34-y}(MeCN)_3(Cd_2Cl_3)]\cdot5MeCN$ (y = 0.61)

The crystal structure of the trianion $[Ni_{36-y}C_8(CO)_{34-y}(MeCN)_3(Cd_2Cl_3)]^{3-}$ was determined by single-crystal X-ray diffraction analysis of its $[Me_4N]_3[Ni_{36-y}C_8(CO)_{34-y}(MeCN)_3(Cd_2Cl_3)]\cdot5MeCN$ (y = 0.61) salt (Figure 2 and Table 1). The fractional indexes are due to the fact that within the same crystal there are two Ni(CO) fragments with refined occupancy factors of 0.688(4) [for Ni(21)C(37)O(37)] and 0.704(3) [for Ni(24)C(19)O(19)].

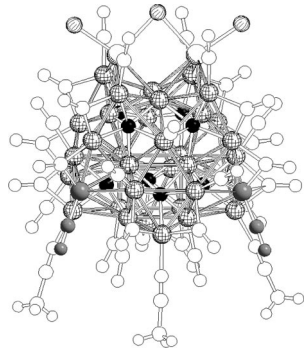

Figure 2. Molecular structure of $[Ni_{36-y}C_8(CO)_{34-y}(MeCN)_3(Cd_2Cl_3)]^{3-}$. Ni: two-direction fully hatched spheres; Cd: semi-hatched spheres; Cl: one-direction fully hatched spheres; interstitial carbide atoms black spheres; Ni(21)C(37)O(37) and Ni(24)C(19)O(19) fragments: grey spheres.

Capping a cluster face with an Ni(CO) group does not alter the electron counting of the molecule, and the possibility of having species that differ only in the presence/absence of such a group is quite common in the chemistry of carbonylnickel clusters.[11,13]

The molecular structure of the $[Ni_{36}C_8(CO)_{34}(MeCN)_3(Cd_2Cl_3)]^{3-}$ trianion is very similar to that of the parent $[Ni_{36}C_8(CO)_{36}(Cd_2Cl_3)]^{5-}$, the bond lengths also being almost identical (Table 1). The most significant differences involve the stereochemistry of the ligands (Figure 3).

In fact, $[Ni_{36}C_8(CO)_{34}(MeCN)_3(Cd_2Cl_3)]^{3-}$ contains 37 ligands, whereas only 36 are present in $[Ni_{36}C_8(CO)_{36}(Cd_2Cl_3)]^{5-}$. As reported above, the latter contains 18 terminal and 18 edge-bridging CO ligands. Conversely, $[Ni_{36}C_8(CO)_{34}(MeCN)_3(Cd_2Cl_3)]^{3-}$ possesses 17 terminal CO, 15 edge-bridging CO, 2 asymmetric edge-bridging CO and 3 MeCN ligands. Of these three, two are coordinated to Ni(29) and Ni(30), replacing the two terminal CO ligands that were present in $[Ni_{36}C_8(CO)_{36}(Cd_2Cl_3)]^{5-}$. The third MeCN molecule is instead added to Ni(36) without

Table 1. Comparison of selected bond lengths [Å] in $[Ni_{36}C_8(CO)_{36}(Cd_2Cl_3)]^{5-}$ and $[Ni_{36-y}C_8(CO)_{34-y}(MeCN)_3(Cd_2Cl_3)]^{3-}$.

	Bond length [Å]	
	$[Ni_{36}C_8(CO)_{36}(Cd_2Cl_3)]^{5-}$	$[Ni_{36-y}C_8(CO)_{34-y}(MeCN)_3(Cd_2Cl_3)]^{3-}$
Ni–Ni	2.3155(14)–3.238(10), av. 2.67	2.3393(14)–3.207(3), av. 2.67
Ni–Cd	2.6543(12)–2.9728(13), av. 2.80	2.6761(12)–2.9222(13), av. 2.82
Ni–C (Oh)[a]	1.874(8)–1.956(8), av. 1.90	1.865(7)–2.003(8), av. 1.90
Ni–C (TP)[b]	1.891(8)–1.953(8), av. 1.92	1.859(8)–1.986(8), av. 1.92
Ni–C (cTP)[c]	1.957(8)–2.175(8), av. 2.01	1.947(8)–2.211(8), av. 2.01
Cd–Cl	2.437(2)–2.599(2), av. 2.52	2.431(3)–2.605(3), av. 2.51
Ni–N	–	1.873(8)–1.901(8), av. 1.89

[a] Relative to the four carbide atoms in distorted octahedral cavities. [b] Relative to the two carbide atoms in trigonal-prismatic cavities. [c] Relative to the two carbide atoms in monocapped trigonal-prismatic cavities.

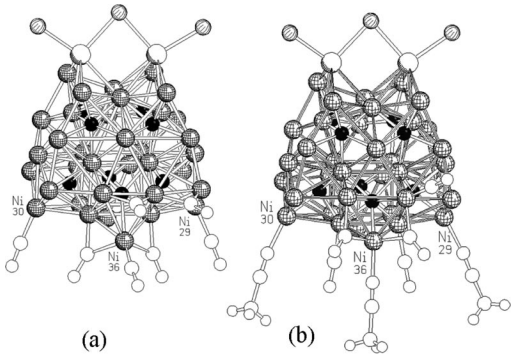

Figure 3. Differences in the stereochemistry of the ligands in (a) $[Ni_{36}C_8(CO)_{36}(Cd_2Cl_3)]^{5-}$ and (b) $[Ni_{36}C_8(CO)_{34}(MeCN)_3(Cd_2Cl_3)]^{3-}$ (all the ligands with a similar coordination in the two species have been omitted). Ni: two-direction fully hatched spheres; Cd: semi-hatched spheres; Cl: one-direction fully hatched spheres; interstitial carbide atoms: black spheres.

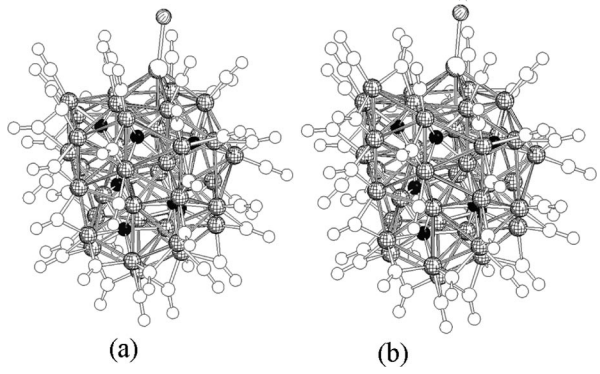

Figure 4. Molecular structures of (a) $[H_{7-n}Ni_{42}C_8(CO)_{44}(CdX)]^{n-}$ and (b) $[H_{7-n}Ni_{43}C_8(CO)_{45}(CdX)]^{n-}$ (n = 6, 7; X = Cl, Br). Ni: two-direction fully hatched spheres; Cd: semi-hatched spheres; Cl: one-direction fully hatched spheres; interstitial carbide atoms: black spheres.

any removal of CO, thereby causing a local rearrangement in the stereochemistry of the carbonyl ligands to create space for the 37th ligand.

Crystal Structures of $[Me_4N]_7[Ni_{42+y}C_8(CO)_{44+y}(CdCl)]\cdot(5-y)MeCN$ (y = 0.19) and $[Me_4N]_6[HNi_{42+y}C_8(CO)_{44+y}(CdBr)]\cdot(6-y)MeCN$ (y = 0.19)

The crystal structures of the two anions $[Ni_{42+y}C_8(CO)_{44+y}(CdCl)]^{7-}$ and $[HNi_{42+y}C_8(CO)_{44+y}(CdBr)]^{6-}$ were determined from analysis of their $[Me_4N]_7[Ni_{42+y}C_8(CO)_{44+y}(CdCl)]\cdot(5-y)MeCN$ (y = 0.19) and $[Me_4N]_6[HNi_{42+y}C_8(CO)_{44+y}(CdBr)]\cdot(6-y)MeCN$ (y = 0.19) salts (Figure 4 and Table 2). Apart from the total charge, the molecular structures of the two anions are almost overlapping.

In both crystals, the asymmetric units contain one cluster anion, the $[Me_4N]^+$ cations (seven and six, respectively) and the MeCN molecules (five and six, respectively). Moreover, in both the anions there is an Ni atom with a partial occupancy factor (ca. 0.19 for both structures). Thus, both crystal structures can be interpreted by assuming in the solid a mixture of two cluster anions, that is, $[H_{7-n}Ni_{42}C_8(CO)_{44}(CdX)]^{n-}$ (main species, ca. 81%) and $[H_{7-n}Ni_{43}C_8(CO)_{45}(CdX)]^{n-}$ (minor species, ca. 19%) (n = 6, 7; X = Cl, Br).

These $[H_{7-n}Ni_{42+y}C_8(CO)_{44+y}(CdX)]^{n-}$ (n = 6, 7; X = Cl, Br; y = 0, 1) clusters display rather complex metal cages, which cannot be described in terms of simple polyhedrons. These structures are, in fact, the result of the condensation of two carbon-centred Ni_6C trigonal prisms, four carbon-centred Ni_7C monocapped trigonal prisms and two carbon-centred Ni_8C square antiprisms. This generates a rather irregular and non-symmetrical $Ni_{38}C_8$ metal carbide cage (Figure 5) in which all Ni atoms are bonded to at least one interstitial carbide atom.

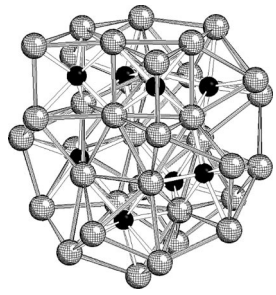

Figure 5. $Ni_{38}C_8$ metal carbide core of $[H_{7-n}Ni_{42+y}C_8(CO)_{44+y}(CdX)]^{n-}$ (n = 6, 7; X = Cl, Br; y = 0, 1). Ni: two-direction fully hatched spheres; interstitial carbide atoms: black spheres.

The addition of five (4 + y) further Ni atoms (which are non-bonded to the interstitial carbide atoms) to this $Ni_{38}C_8$ metal cage results in the final $Ni_{42+y}C_8$ structure. The unique $[CdX]^+$ unit is coordinated to an almost planar pentagonal face of the $Ni_{42+y}C_8$ cage. On the surface of the cluster there are 45 carbonyl ligands of which 19 are terminal, 25 are edge-bridging and one face-bridging for the

Table 2. Comparison of selected bond lengths [Å] in $[Ni_{42+y}C_8(CO)_{44+y}(CdCl)]^{7-}$ and $[HNi_{42+y}C_8(CO)_{44+y}(CdBr)]^{6-}$.

	Bond length [Å]	
	$[Ni_{42+y}C_8(CO)_{44+y}(CdCl)]^{7-}$	$[HNi_{42+y}C_8(CO)_{44+y}(CdBr)]^{6-}$
Ni–Ni	2.330(9)–3.281(2), av. 2.63	2.3511(17)–3.287(2), av. 2.62
Ni–Cd	2.6962(13)–2.8276(12), av. 2.73	2.6954(15)–2.8136(15), av. 2.73
Ni–C (S-A)[a]	1.956(8)–2.230(8), av. 2.06	1.957(10)–2.226(10), av. 2.05
Ni–C (TP)[b]	1.878(8)–2.027(9), av. 1.93	1.879(10)–2.030(10), av. 1.93
Ni–C (cTP)[c]	1.917(8)–2.136(8), av. 2.00	1.904(10)–2.153(10), av. 1.99
Cd(1)–Br(1)		2.5502(16)
Cd(1)–Cl(1)	2.467(3)	

[a] For the carbide atoms in square anti-prismatic cages. [b] For the carbide atoms in trigonal-prismatic cages. [c] For the carbide atoms in monocapped trigonal-prismatic cages.

minor species $[H_{7-n}Ni_{43}C_8(CO)_{45}(CdX)]^{n-}$ (n = 6, 7; X = Cl, Br), and 21 are terminal, 22 are edge-bridging and one face-bridging (total 44) for the major species $[H_{7-n}Ni_{42}C_8(CO)_{44}(CdX)]^{n-}$ (n = 6, 7; X = Cl, Br).

Electrochemical and Spectroelectrochemical Studies

It has been shown previously that the Ni–Cd tetracarbide MCC $[Ni_{30}C_4(CO)_{34}(CdCl)_2]^{6-}$ in dmf solution displays several reversible redox processes.[12] Electrochemical studies in CH_3CN are complicated by the occurrence of protonation equilibria. Similar results have now also been found for the octacarbide species $[H_{5-n}Ni_{36}C_8(CO)_{36}(Cd_2Cl_3)]^{n-}$ (n = 3–5) and $[H_{7-n}Ni_{42+y}C_8(CO)_{44+y}(CdCl)]^{n-}$ (n = 6, 7; y = 0, 1) reported herein as well as for the previously reported tetraacetylide $[H_{4-n}Ni_{22}(C_2)_4(CO)_{28}(CdBr)_2]^{n-}$ (n = 2–4; Table 3).

As illustrated in Figure 6a, the cyclic voltammetric response of $[Ni_{36}C_8(CO)_{36}(Cd_2Cl_3)]^{5-}$ exhibits one oxidation as well as two main reductions, displaying chemical reversibility on the cyclic voltammetric timescale, as better shown by deconvolution of the cyclic voltammogram (Figure 6b).

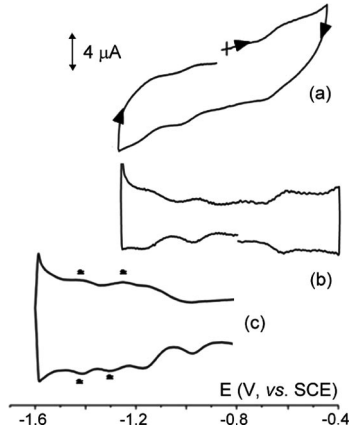

Figure 6. (a) Cyclic voltammetric profile recorded at a glassy carbon electrode in a saturated dmf solution of $[Me_4N]_5[Ni_{36}C_8(CO)_{36}(Cd_2Cl_3)]$. (b) (c) First-derivative deconvoluted voltammmograms. $[Et_4N][PF_6]$ (0.1 mol dm^{-3}) as supporting electrolyte. Scan rate 0.2 V s^{-1}.

Because the very small current intensities due to both the very low diffusion coefficient of the high-nuclearity cluster and its limited solubility prevented any experimental measurement of the number of electrons involved in the different redox processes, we confidently assigned them to one-electron processes.

Figure 6c also shows that two more cathodic processes (asterisked peak systems) are present, which are attributed to by-products arising from the chemical complications accompanying the second main reduction. In fact, analysis of the cyclic voltammograms with scan rates progressively increasing from 0.02 to 0.5 V s^{-1} indicates that the oxidation and the first reduction processes are chemically and electrochemically reversible, whereas the second reduction is accompanied by chemical complications (as suggested by the value of the i_{pa}/i_{pc} ratio, which increases from 0.5 at 0.05 V s^{-1} to 1 at 0.2 V s^{-1}).[19] Based on the appearance of the typical ν_{CO} band at 1891 cm^{-1} in the IR spectra, such chemical complications are assigned to the partial fragmentation of the original cluster to $[Ni_{32}C_6(CO)_{36}]^{6-}$.[11d]

Finally, further cathodic processes (not shown in Figure 6), with marked high peak heights and features of partial chemical reversibility, are also present at rather negative potentials ($E^{\circ\prime}$ = –1.66 and –1.80 V, respectively), which show in the reverse scan a stripping anodic peak. Based on such a feature, such cathodic processes are confidently assigned to the Cd^{2+}/Cd^0 step followed by the release of Cd metal, as previously detected for $[Ni_{30}C_4(CO)_{34}(CdCl)_2]^{6-}$.[12]

As far as the IR spectroelectrochemical investigation at the first reduction process is concerned, the progressive disappearance of the terminal ν^t_{CO} band at 2004 cm^{-1} in favour of the new stretching band at 1985 cm^{-1}, attributable to $[Ni_{36}C_8(CO)_{36}(Cd_2Cl_3)]^{6-}$, is accompanied by the formation of the isosbestic point at 1992 cm^{-1} (Figure 7a). Upon an-

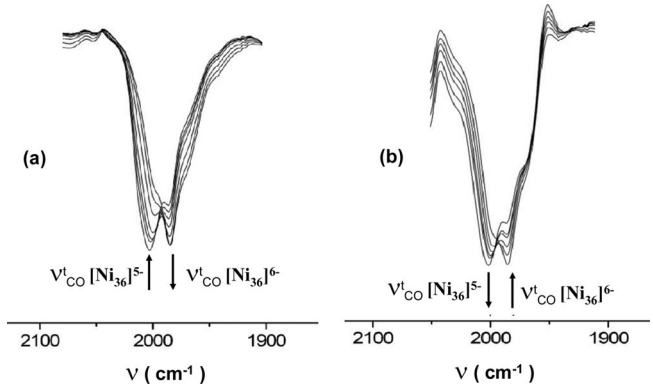

Figure 7. IR spectroelectrochemical trends recorded in the region of the terminal ν_{CO} frequencies for $[Me_4N]_5[Ni_{36}C_8(CO)_{36}(Cd_2Cl_3)]$ in dmf solution by using an OTTLE cell. (a) Stepwise variation of the potential from E_w = –0.70 to –1.15 V vs. pseudo-reference Ag electrode. (b) Reoxidation from E_w = –1.15 to –0.70 V. $[Et_4N][PF_6]$ (0.1 mol dm^{-3}) as the supporting electrolyte.

Table 3. Formal electrode potentials (vs. SCE) for the redox changes exhibited by $[Ni_{30}C_4(CO)_{34}(CdCl)_2]^{6-}$, $[Ni_{36}C_8(CO)_{36}(Cd_2Cl_3)]^{5-}$, $[HNi_{42+y}C_8(CO)_{44+y}(CdCl)]^{6-}$ and $[Ni_{22}(C_2)_4(CO)_{28}(CdBr)_2]^{4-}$ in dmf solution.

	$E^{\circ\prime}_{4-/5-}$ [V]	$E^{\circ\prime}_{5-/6-}$ [V]	$E^{\circ\prime}_{6-/7-}$ [V]	$E^{\circ\prime}_{7-/8-}$ [V]	$E^{\circ\prime}_{8-/9-}$ [V]
$[Ni_{30}C_4(CO)_{34}(CdCl)_2]^{6-}$[a]	–	–0.49	–0.88	–1.28	–
$[Ni_{36}C_8(CO)_{36}(Cd_2Cl_3)]^{5-}$	–0.61	–0.97	–1.15	–	
$[HNi_{42+y}C_8(CO)_{44+y}(CdCl)]^{6-}$	–	–0.45	–0.70	–0.91	–1.18
$[Ni_{22}(C_2)_4(CO)_{28}(CdBr)_2]^{4-}$	–0.71	–0.85	–	–	

[a] From ref.[12]

odic reoxidation, $[Ni_{36}C_8(CO)_{36}(Cd_2Cl_3)]^{6-}$ is reversibly converted into $[Ni_{36}C_8(CO)_{36}(Cd_2Cl_3)]^{5-}$ (Figure 7b).

Concerning the tetraanion $[HNi_{36}C_8(CO)_{36}(Cd_2Cl_3)]^{4-}$, the voltammetric profile in CH_3CN solution looks more complex than that of the pentaanion $[Ni_{36}C_8(CO)_{36}(Cd_2Cl_3)]^{5-}$ because of the occurrence in solution of protonation–deprotonantion equilibria (Scheme 2). Note, however, that also in this case redox-reversible processes are observed, which, as shown in Figure S1 in the Supporting Information, are split into two closely spaced peak systems as a mixture of $[HNi_{36}C_8(CO)_{36}(Cd_2Cl_3)]^{4-}$ and $[Ni_{36}C_8(CO)_{36}(Cd_2Cl_3)]^{5-}$ is actually present in solution (in fact, the observed peaks are very close to the ones observed for the pentaanion in dmf solution). In fact, the IR spectra in CH_3CN solution suggest that $[HNi_{36}C_8(CO)_{36}(Cd_2Cl_3)]^{4-}$ is the prevailing species in solution ($\tilde{\nu}^t_{CO}$ = 2014 cm^{-1}). In addition, spectroelectrochemical studies confirm its reversible reduction to $[HNi_{36}C_8(CO)_{36}(Cd_2Cl_3)]^{5-}$ ($\tilde{\nu}^t_{CO}$ = 1990 cm^{-1}), as supported by the appearance of an isosbestic point at 2000 cm^{-1} (see Figure S2 in the Supporting Information).

As illustrated in Figure 8, the hexaanion $[HNi_{42+y}C_8(CO)_{44+y}(CdCl)]^{6-}$ displays a series of (probably one-electron) processes, namely, one oxidation (not shown in the figure) and three reduction processes showing features of chemical reversibility. Also, in this case, the further reduction process due to the Cd^{II}/Cd^0 process is present at very negative potential values ($E°'$ = –1.99 V).

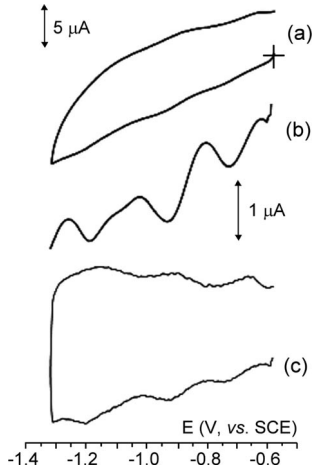

Figure 8. (a) Cyclic, (b) Osteryoung square-wave and (c) deconvoluted voltammograms recorded at a glassy carbon electrode in a saturated dmf solution of $[Me_4N]_6[HNi_{42+y}C_8(CO)_{44+y}(CdCl)]$. $[Et_4N][PF_6]$ (0.1 mol dm^{-3}) as the supporting electrolyte. Scan rates: (a) 0.02 V s^{-1}; (b) 0.1 V s^{-1}.

Spectroelectrochemical studies of the first reduction shows that the original ν^t_{CO} band at 2009 cm^{-1} is converted into a new species displaying a ν^t_{CO} band at 1973 cm^{-1} (see Figure S3 in the Supporting Information). The reversibility of the reduction process, as proven by the appearance of the isosbestic point at 1987 cm^{-1}, suggests that this new species is the heptaanion $[HNi_{42+y}C_8(CO)_{44+y}(CdCl)]^{7-}$.

Let us finally pass to the anions $[H_{4-n}Ni_{22}(C_2)_4(CO)_{28}(CdBr)_2]^{n-}$ (n = 2–4), the synthesis and structures of which have previously been reported.[14] In thf solution the prominent form is $[H_2Ni_{22}(C_2)_4(CO)_{28}(CdBr)_2]^{2-}$, which, in dmf deprotonates and is converted into the tetraanion $[Ni_{22}(C_2)_4(CO)_{28}(CdBr)_2]^{4-}$ (see Figure S4 in the Supporting Information).[14] Note that in this case the presence and number of hydride atoms was fully confirmed by ^1H NMR spectroscopy.

Figure 9 allows a comparison of the voltammetric profiles of the dianion $[H_2Ni_{22}(C_2)_4(CO)_{28}(CdBr)_2]^{2-}$ in thf solution (Figure 9a) with that of its deprotonated tetraanion $[Ni_{22}(C_2)_4(CO)_{28}(CdBr)_2]^{4-}$ in dmf solution (Figure 9b).

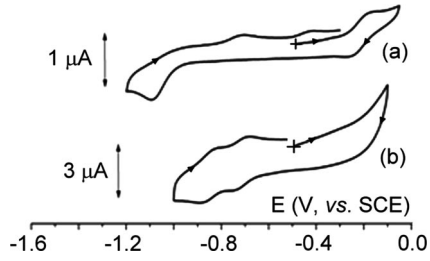

Figure 9. Cyclic voltammetric profiles recorded in (a) a saturated thf solution of $[H_2Ni_{22}(C_2)_4(CO)_{28}(CdBr)_2]^{2-}$ and (b) a dmf solution of $[Ni_{22}(C_2)_4(CO)_{28}(CdBr)_2]^{4-}$ (0.7×10^{-3} mol dm^{-3}). $[Bu_4N][PF_6]$ (0.2 mol dm^{-3}) as the supporting electrolyte. (a) Platinum electrode; scan rate 0.05 V s^{-1}. (b) Glassy carbon electrode; scan rate 0.10 V s^{-1}.

In thf solution the protonated dianion exhibits one oxidation showing features of chemical reversibility ($E°'$ = –0.21 V) and one irreversible reduction at E_p = –1.08 V. In addition, not shown in Figure 10, a partially reversible cathodic step is present at $E°'$ = –1.52 V, which, displaying a stripping anodic peak in the reverse scan, is confidently assigned to the Cd^{2+}/Cd^0 process. In dmf solution, the deprotonated tetraanion exhibits two closely spaced reversible reductions.

As illustrated in Figure 10, the spectroelectrochemical trend recorded upon progressive oxidation of $[H_2Ni_{22}(C_2)_4(CO)_{28}(CdBr)_2]^{2-}$ in thf solution shows that the original ν^t_{CO} band at 2025 cm^{-1} is converted into a new species displaying a ν^t_{CO} band at 2035 cm^{-1}. The appearance of the isosbestic point at 2029 cm^{-1} suggests that such a new species is likely the monoanion $[H_2Ni_{22}(C_2)_4(CO)_{28}(CdBr)_2]^{-}$.

As far as the reduction processes of $[Ni_{22}(C_2)_4(CO)_{28}(CdBr)_2]^{4-}$ in dmf solution are concerned, the spectroelectrochemical trend illustrated in Figure 11 confirms the formation of the corresponding penta- and hexaanions, as proven by the appearance of the isosbestic point at 1990 cm^{-1} between the ν^t_{CO} band of $[Ni_{22}(C_2)_4(CO)_{28}(CdBr)_2]^{4-}$ (2004 cm^{-1}) and that of $[Ni_{22}(C_2)_4(CO)_{28}(CdBr)_2]^{5-}$ (1986 cm^{-1}) and the isosbestic point at 1977 cm^{-1} between the ν^t_{CO} band of $[Ni_{22}(C_2)_4(CO)_{28}(CdBr)_2]^{5-}$ (1986 cm^{-1}) and that of $[Ni_{22}(C_2)_4(CO)_{28}(CdBr)_2]^{6-}$ (1968 cm^{-1}).

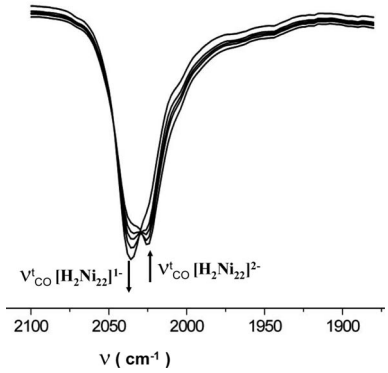

Figure 10. IR spectra (in the stretching region of terminal CO frequencies) recorded in an OTTLE cell upon progressive anodic oxidation of $[H_2Ni_{22}(C_2)_4(CO)_{28}(CdBr)_2]^{2-}$ in thf solution. $[Bu_4N][PF_6]$ (0.2 mol dm^{-3}) as the supporting electrolyte. Potential range from E_w = –0.30 to +0.15 V (vs. pseudo-reference Ag electrode).

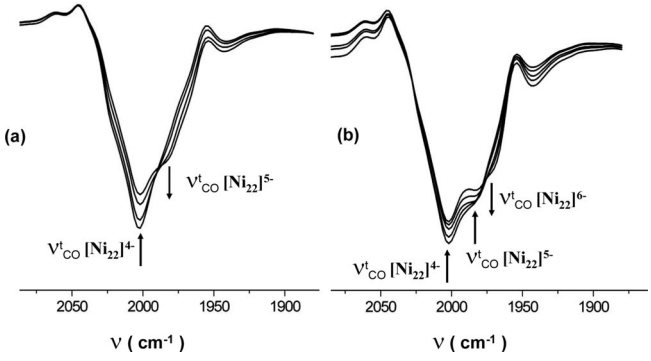

Figure 11. IR spectra (in the stretching region of terminal CO frequencies) recorded in an OTTLE cell upon progressive cathodic reductions of $[Ni_{22}(C_2)_4(CO)_{28}(CdBr)_2]^{4-}$ in dmf solution. $[Bu_4N][PF_6]$ (0.2 mol dm^{-3}) as the supporting electrolyte. Potential range: (a) E_w = –0.50 to –0.85 V; (b) from E_w = –0.85 to –1.50 V (vs. pseudo-reference Ag electrode).

To confirm the stability of the deprotonated penta- and hexaanions, the progressive reoxidation regenerates the original spectrum of $[Ni_{22}(C_2)_4(CO)_{28}(CdBr)_2]^{4-}$ (Figure S5 in the Supporting Information).

Conclusions

The first examples of Ni octacarbide MCCs have been described herein. This work completes our description of the Ni–Cd carbide heterodimetallic MCC system and shows the possibility of obtaining tetra- and octacarbide species as well as tetraacetylide clusters.[12–14]

Other remarkable features are the nearly systematic tendency in high-nuclearity MCCs of displaying polyhydride character and the fact that very often capping Ni(CO) fragments are partially vacant in Ni MCCs. The first point has been widely discussed in a recent paper together with the major problems of directly proving the presence of hydride ligands in high-nuclearity MCCs by ^{1}H NMR spectroscopy.[14] Regarding the second point, this is very specific of Ni clusters, which very often cannot be described as single species but are better described as families of clusters differing by a few Ni(CO) groups. Owing to the high nuclearity of these MCCs, species belonging to the same family display almost identical physical properties, as evidenced by IR and electrochemical studies. Moreover, these two points make the description of molecular Ni MCCs rather complicated, as already evident from the fact that they require very complex molecular formulae that may contain fractional indexes. These considerations indicate that a detailed description of molecular species containing a few dozen metal atoms is rather troublesome and non-trivial. Thus, a satisfactory description of large metal clusters at the molecular level can be achieved only by combining several different techniques, such as X-ray diffraction, IR, NMR (when possible), as well as chemical and electrochemical investigations. This conclusion should be kept in mind when dealing with larger and non-molecular species such as metal nanoparticles and colloids.

Finally, this work confirms that Ni carbide MCCs have a very rich and variegated chemistry. Mono-, tetra-, hexa- and octacarbide species are formed as well as mono-, di- and tetraacetylides. All these species display very complex and irregular metal cages, which are required to accommodate the isolated C atoms or C_2 units. This behaviour confirms that the metal core in ligand-stabilised clusters is rather deformable and soft: it behaves more like a liquid metal drop that adapts itself to the surface and/or interstitial ligands rather than a solid close-packed metal chunk. It is, therefore, not surprising that the diffusion and mobility of carbon atoms into "nearly liquid" Fe, Co and Ni nanoparticles have been claimed as the basis of the growth of carbon nanotubes promoted by these catalysts.[20] A further remarkable aspect is their marked redox activity, which is often manifested by sequences of reversible oxidation/reduction processes.

Experimental Section

General: All reactions and sample manipulations were carried out by using standard Schlenk techniques under nitrogen and in dried solvents. All the reagents were commercial products (Aldrich) of the highest purity available and used as received. The $[Me_4N]_2[Ni_{10}C_2(CO)_{15}]$[17] salt was prepared according to a literature procedure. Analyses of Ni and Cd were performed by atomic absorption spectroscopy with a Pye-Unicam instrument. Analyses of C, H and N were performed with a ThermoQuest FlashEA 1112NC instrument. IR spectra were recorded with a Perkin–Elmer SpectrumOne interferometer in CaF_2 cells. ^{1}H NMR spectra were recorded with Varian Gemini 400 MHz and Varian Inova 600 MHz spectrometers and are referenced to internal TMS. Structures were drawn with SCHAKAL99.[21] Materials and apparatus for electrochemistry and spectroelectrochemistry have been described elsewhere.[22] Under the present experimental conditions, the one-electron oxidation of ferrocene occurs at $E°'$ = +0.47 V in dmf solution, $E°'$ = +0.49 V in thf solution and +0.38 V in MeCN solution.

Synthesis of $[Me_4N]_5[Ni_{36}C_8(CO)_{36}(Cd_2Cl_3)]\cdot(7–2y)MeCN\cdot yC_6H_{14}$ (y = 0.40): $CdCl_2\cdot 2.5H_2O$ (1.12 g, 4.90 mmol) was added to a solution of $[Me_4N]_2[Ni_{10}C_2(CO)_{15}]$ (0.68 g, 0.577 mmol) in thf (20 mL)

with stirring. The mixture was left to react for 3 h until all the starting $[Me_4N]_2[Ni_{10}C_2(CO)_{15}]$ had disappeared (IR monitoring), and then the resulting dark-brown suspension was concentrated to dryness. The residue was washed with water (40 mL) and carefully dried under vacuum. The dihydride trianion $[H_2Ni_{36}C_8(CO)_{36}(Cd_2Cl_3)]^{3-}$ was extracted from the residue in thf (20 mL) and deprotonated to give the monohydride tetraanion $[HNi_{36}C_8(CO)_{36}(Cd_2Cl_3)]^{4-}$ after evaporating the solvent in vacuo and dissolution in MeCN (20 mL). Precipitation by slow diffusion of *n*-hexane (5 mL) and diisopropyl ether (40 mL) gave a dark-brown crystalline precipitate composed of crystals of $[Me_4N]_5[Ni_{36}C_8(CO)_{36}(Cd_2Cl_3)]\cdot(7–2y)MeCN\cdot yC_6H_{14}$ due to further deprotonation during crystallisation (yield: 0.498 g, 73.8% based on Ni). The salt is soluble in thf, acetone, acetonitrile, dmf and dmso, insoluble in less-polar solvents. The compound is present as the dihydride trianion $[H_2Ni_{36}C_8(CO)_{36}(Cd_2Cl_3)]^{3-}$ in thf and acetone, whereas it is deprotonated to the monohydride tetraanion $[HNi_{36}C_8(CO)_{36}(Cd_2Cl_3)]^{4-}$ in acetonitrile and to the pentaanion $[Ni_{36}C_8(CO)_{36}(Cd_2Cl_3)]^{5-}$ in dmf. $C_{78.80}H_{84.20}Cd_2Cl_3N_{11.20}Ni_{36}O_{36}$ (4208.999): calcd. C 22.49, H 2.02, N 3.73, Ni 50.21, Cd 5.34; found C 22.36, H 2.19, N 3.58, Ni 50.45, Cd 5.12. $[H_2Ni_{36}C_8(CO)_{36}(Cd_2Cl_3)]^{3-}$: IR (thf, 293 K): $\tilde{\nu}_{CO}$ = 2030 (s), 1854 (m) cm^{-1}. $[HNi_{36}C_8(CO)_{36}(Cd_2Cl_3)]^{4-}$: IR (MeCN, 293 K): $\tilde{\nu}_{CO}$ = 2014 (s), 1856 (br.) cm^{-1}. $[Ni_{36}C_8(CO)_{36}(Cd_2Cl_3)]^{5-}$: IR (dmf 293 K): $\tilde{\nu}_{CO}$ = 2004 (s), 1846 (m) cm^{-1}.

Synthesis of $[Me_4N]_3[Ni_{36-y}C_8(CO)_{34-y}(MeCN)_3(Cd_2Cl_3)]\cdot5MeCN$ (y = 0.61): A solution of $[HNi_{36}C_8(CO)_{36}(Cd_2Cl_3)]^{4-}$ (0.118 mmol) in MeCN (30 mL) was stirred at room temperature for 1 week. The solvent was then removed in vacuo and the residue washed with water (40 mL) and extracted in MeCN (20 mL). Precipitation by slow diffusion of *n*-hexane (5 mL) and diisopropyl ether (40 mL) gave a dark-brown crystalline precipitate composed of crystals of $[Me_4N]_3[Ni_{36-y}C_8(CO)_{34-y}(MeCN)_3(Cd_2Cl_3)]\cdot5MeCN$ (y = 0.61) and an amorphous solid containing unreacted $[HNi_{36}C_8(CO)_{36}(Cd_2Cl_3)]^{4-}$. As a result of difficulties in separating the two species, it was not possible to further characterise the compound, apart from X-ray analysis of a single crystal.

Synthesis of $[Me_4N]_7[Ni_{42+y}C_8(CO)_{44+y}(CdCl)]\cdot(5–y)MeCN$ (y = 0.19): NaOH (0.65 g, 16.25 mmol) was added to a solution of $[Me_4N]_5[Ni_{36}C_8(CO)_{36}(Cd_2Cl_3)]\cdot(7–2y)MeCN\cdot yC_6H_{14}$ (0.47 g, 0.112 mmol) in MeCN (20 mL) and the resulting suspension stirred overnight. The mixture was then filtered to remove the excess NaOH, the solvent was removed in vacuo and the residue washed with water (40 mL). The $[HNi_{42+y}C_8(CO)_{44+y}(CdCl)]^{6-}$ hexaanion was extracted in MeCN (20 mL) from the residue, and crystals of $[Me_4N]_7[Ni_{42+y}C_8(CO)_{44+y}(CdCl)]\cdot(5–y)MeCN$ (y = 0.19) suitable for X-ray analysis were obtained by slow diffusion of *n*-hexane (5 mL) and diisopropyl ether (40 mL) (yield: 0.26 g, 59% based on Ni). As evidenced by the X-ray analysis, deprotonation of the hexaanion to give the heptaanion occurs during crystallisation; and vice versa, dissolution of the crystals in MeCN or dmf is accompanied by protonation, and therefore in solution only the IR spectrum of $[HNi_{42+y}C_8(CO)_{44+y}(CdCl)]^{6-}$ was observed. $C_{89.81}H_{98.42}CdClN_{11.81}Ni_{42.19}O_{44.19}$ (4675.39): calcd. C 23.08, H 2.12, N 3.54, Ni 52.97, Cd 2.40; found C 23.26, H 2.01, N 3.71, Ni 53.05, Cd 2.22. $[HNi_{44+y}C_8(CO)_{44+y}(CdCl)]^{6-}$: IR (MeCN, 293 K): $\tilde{\nu}_{CO}$ = 2004 (s), 1847 (m) cm^{-1}; (dmf, 293 K): $\tilde{\nu}_{CO}$ = 2002 (s), 1850 (m) cm^{-1}. $[Ni_{44+y}C_8(CO)_{44+y}(CdCl)]^{7-}$: IR (Nujol mull, 293 K): $\tilde{\nu}_{CO}$ = 2000 (w), 1975 (vs), 1833 (ms), 1779 (m) cm^{-1}.

Synthesis of $[Me_4N]_6[HNi_{42+y}C_8(CO)_{44+y}(CdBr)]\cdot(6–y)MeCN$ (y = 0.19): NaOH (0.65 g, 16.25 mmol) was added to a solution of $[Me_4N]_5[Ni_{36}C_8(CO)_{36}(Cd_2Br_3)]\cdot(7–2y)MeCN\cdot yC_6H_{14}$ (0.52 g, 0.120 mmol) in MeCN (20 mL) and the resulting suspension stirred overnight. The mixture was then filtered to remove the excess NaOH, the solvent was removed in vacuo and the residue washed with water (40 mL). The $[HNi_{42+y}C_8(CO)_{44+y}(CdBr)]^{6-}$ hexaanion was extracted in MeCN (20 mL) from the residue, and crystals of $[Me_4N]_6[HNi_{42+y}C_8(CO)_{44+y}(CdBr)]\cdot(6–y)MeCN$ (y = 0.19) suitable for X-ray analysis were obtained by slow diffusion of *n*-hexane (5 mL) and diisopropyl ether (40 mL; yield: 0.30 g, 62% based on Ni). $C_{87.81}H_{89.43}BrCdN_{11.81}Ni_{42.19}O_{44.19}$ (4686.52): calcd. C 22.51, H 1.92, N 3.53, Ni 52.85, Cd 2.40; found C 22.32, H 1.83, N 3.21, Ni 53.06, Cd 2.57. $[HNi_{44+y}C_8(CO)_{44+y}(CdBr)]^{6-}$: IR (MeCN, 293 K): $\tilde{\nu}_{CO}$ = 2009 (s), 1851 (m) cm^{-1}; (dmf, 293 K): $\tilde{\nu}_{CO}$ = 2002 (s), 1850 (m) cm^{-1}.

X-ray Crystallographic Study: Crystal data and collection details for $[Me_4N]_5[Ni_{36}C_8(CO)_{36}(Cd_2Cl_3)]\cdot(7–2y)MeCN\cdot yC_6H_{14}$ (y = 0.40), $[Me_4N]_3[Ni_{36-y}C_8(CO)_{34-y}(MeCN)_3(Cd_2Cl_3)]\cdot5MeCN$ (y = 0.61), $[Me_4N]_7[Ni_{42+y}C_8(CO)_{44+y}(CdCl)]\cdot(5–y)MeCN$ (y = 0.19) and $[Me_4N]_6[HNi_{42+y}C_8(CO)_{44+y}(CdBr)]\cdot(6–y)MeCN$ (y = 0.19) are reported in Table 4. The diffraction experiments were performed with a Bruker APEX II diffractometer equipped with a CCD detector by using Mo-K_α radiation. Data were corrected for Lorentz polarization and absorption effects (empirical absorption correction SADABS).[23] Structures were solved by direct methods and refined by full-matrix least squares based on all data by using F^2.[24] Hydrogen atoms were fixed at calculated positions and refined by a riding model. All non-hydrogen atoms were refined with anisotropic displacement parameters unless otherwise stated. CCDC-773550 {for $[Me_4N]_5[Ni_{36}C_8(CO)_{36}(Cd_2Cl_3)]\cdot(7–2y)MeCN\cdot yC_6H_{14}$}, -773551 {for $[Me_4N]_3[Ni_{36-y}C_8(CO)_{34-y}(MeCN)_3(Cd_2Cl_3)]\cdot5MeCN$}, -773808 {for $[Me_4N]_6[HNi_{42+y}C_8(CO)_{44+y}(CdBr)]\cdot(6–y)MeCN$} and -773809 {for $[Me_4N]_7[Ni_{42+y}C_8(CO)_{44+y}(CdCl)]\cdot(5–y)MeCN$} contain the supplementary crystallographic data for this paper. These data can be obtained free of charge from The Cambridge Crystallographic Data Centre via www.ccdc.cam.ac.uk/data_request/cif.

$[Me_4N]_5[Ni_{36}C_8(CO)_{36}(Cd_2Cl_3)]\cdot(7–2y)MeCN\cdot yC_6H_{14}$ (y = 0.40): The asymmetric unit contains the cluster anion, five independent $[Me_4N]^+$ cations, seven MeCN molecules and one *n*-hexane molecule all located in general positions. Substitutional disorder exists between two of the MeCN molecules and one *n*-hexane molecule; their occupancy factor was refined [0.600(10) for the two MeCN molecules] by using the PART instruction of SHELX97.[24] Disordered groups were refined isotropically. Similar U restraints were applied to the C, O and N atoms.

$[Me_4N]_3[Ni_{36-y}C_8(CO)_{34-y}(MeCN)_3(Cd_2Cl_3)]\cdot5MeCN$ (y = 0.61): The asymmetric unit contains the cluster anion, three independent $[Me_4N]^+$ cations and five MeCN molecules all located in general positions. The Ni(21)C(37)O(37) and Ni(24)C(19)O(19) groups have refined occupancy factors of 0.688(4) and 0.704(3), respectively. One MeCN molecule appears to be disordered over two positions; disordered atomic positions were split and refined by using one occupancy parameter per disordered group. All cations and MeCN molecules were refined isotropically. Similar U restraints were applied to the C, O, N, Cl and Ni atoms; the ISOR restraint of SHELX97[24] was applied to some of the O atoms of the carbonyl ligands. Restrained bond lengths were applied to the CO ligands, the MeCN molecules and the $[Me_4N]^+$ cations.

$[Me_4N]_7[Ni_{42+y}C_8(CO)_{44+y}(CdCl)]\cdot(5–y)MeCN$ (y = 0.19): The asymmetric unit contains the cluster anion, seven independent $[Me_4N]^+$ cations and five MeCN molecules all located in general positions. The Ni(44)C(54)O(54) group has a partial occupancy factor [0.184(3) after refinement]. To improve the model, the CO ligands bridging towards Ni(44) were also split. PART 1 of the

Table 4. Crystal data and experimental details for $[Me_4N]_5[Ni_{36}C_8(CO)_{36}(Cd_2Cl_3)]\cdot(7–2y)MeCN\cdot yC_6H_{14}$ (y = 0.40), $[Me_4N]_3[Ni_{36-y}C_8(CO)_{34-y}(MeCN)_3(Cd_2Cl_3)]\cdot 5MeCN$ (y = 0.61), $[Me_4N]_7[Ni_{42+y}C_8(CO)_{44+y}(CdCl)]\cdot(5–y)MeCN$ (y = 0.19) and $[Me_4N]_6[HNi_{42+y}C_8(CO)_{44+y}(CdBr)]\cdot(5–y)MeCN$ (y = 0.19).

	$[Me_4N]_5[Ni_{36}C_8(CO)_{36}(Cd_2Cl_3)]\cdot(7–2y)MeCN\cdot yC_6H_{14}$	$[Me_4N]_3[Ni_{36-y}C_8(CO)_{34-y}(MeCN)_3(Cd_2Cl_3)]\cdot 5MeCN$
Empirical formula	$C_{78.80}H_{84.20}Cd_2Cl_3N_{11.20}Ni_{36}O_{36}$	$C_{69.39}H_{60}Cd_2Cl_3N_{11}Ni_{35.39}O_{33.39}$
M_r	4208.999	3991.10
T [K]	100(2)	295(2)
λ [Å]	0.71073	0.71073
Crystal system	monoclinic	triclinic
Space group	$P2_1/n$	$P\bar{1}$
a [Å]	15.6650(9)	14.3520(17)
b [Å]	43.672(3)	17.311(2)
c [Å]	18.0838(10)	24.771(3)
α [°]	90	81.093(2)
β [°]	105.4880(10)	87.295(2)
γ [°]	90	69.315(2)
Cell volume [Å^3]	11922.2(12)	5688.2(12)
Z	4	2
D_c [g cm^{-3}]	2.345	2.330
μ [mm^{-1}]	6.014	6.198
F(000)	8314	3917
Crystal size [mm]	0.21 × 0.16 × 0.12	0.23 × 0.18 × 0.12
θ limits [°]	1.49–25.03	1.41–25.03
Index ranges	$-18 \le h \le 18$	$-17 \le h \le 17$
	$-51 \le k \le 51$	$-20 \le k \le 20$
	$-21 \le l \le 21$	$-29 \le l \le 29$
Reflections collected	113203	54581
Independent reflections	21061 (R_{int} = 0.0665)	20044 (R_{int} = 0.0579)
Completeness to θ = 25.03° [%]	99.9	99.7
Data/restraints/parameters	21061/67/1499	20044/384/1270
Goodness of fit on F^2	1.139	1.060
R_1 [$I > 2\sigma(I)$]	0.04842	0.0476
wR_2 (all data)	0.0964	0.1380
Largest diff. peak/hole [e Å^{-3}]	1.672/–1.425	1.117/–2.157
	$[Me_4N]_7[Ni_{42+y}C_8(CO)_{44+y}(CdCl)]\cdot(5–y)MeCN$	$[Me_4N]_6[HNi_{42+y}C_8(CO)_{44+y}(CdBr)]\cdot(6–y)MeCN$
Empirical formula	$C_{89.81}H_{98.42}CdClN_{11.81}Ni_{42.19}O_{44.19}$	$C_{87.81}H_{89.43}BrCdN_{11.81}Ni_{42.19}O_{44.19}$
M_r	4675.39	4686.52
T [K]	100(2)	100(2)
λ [Å]	0.71073	0.71073
Crystal system	monoclinic	monoclinic
Space group	$P2_1/n$	$P2_1/n$
a [Å]	16.0467(11)	15.7557(19)
b [Å]	31.469(2)	31.042(4)
c [Å]	26.4957(18)	26.199(3)
α [°]	90	90
β [°]	94.8650(10)	95.530(2)
γ [°]	90	90
Cell volume [Å^3]	13331.3(16)	12754(3)
Z	4	4
D_c [g cm^{-3}]	2.329	2.441
μ [mm^{-1}]	6.044	6.609
F(000)	9280	9267
Crystal size [mm]	0.24 × 0.21 × 0.16	0.19 × 0.15 × 0.12
θ limits [°]	1.43–25.03	1.02–27.00
Index ranges	$-19 \le h \le 19$	$-20 \le h \le 20$
	$-37 \le k \le 37$	$-39 \le k \le 39$
	$-31 \le l \le 31$	$-33 \le l \le 33$
Reflections collected	126127	139003
Independent reflections	23507 (R_{int} = 0.0654)	27844 (R_{int} = 0.0755)
Completeness to θ = 25.03° [%]	99.8	100.0
Data/restraints/parameters	23507/380/1625	27844/3834/1636
Goodness of fit on F^2	1.038	1.089
R_1 [$I > 2\sigma(I)$]	0.0490	0.0696
wR_2 (all data)	0.1367	0.1774
Largest diff. peak/hole [e Å^{-3}]	4.260/–1.685	3.266/–2.0468

model contains Ni(44), C(54), O(54), C(56), O(56), C(57) and O(57), whereas PART 2 contains C(10), O(10), C(25), O(25) and one non-coordinated MeCN molecule. Disordered carbonyl ligands as well as all MeCN molecules were refined isotropically. Similar *U* restraints were applied to the C, O and N atoms; the ISOR restraint of SHELX97[24] was applied to some of the O atoms of the carbonyl ligands and three of the $[Me_4N]^+$ cations. Restrained bond lengths were applied to the CO ligands, the MeCN molecules and the $[Me_4N]^+$ cations.

$[Me_4N]_6[HNi_{42+y}C_8(CO)_{44+y}(CdBr)]\cdot(6–y)MeCN$ (y = 0.19): The asymmetric unit contains the cluster anion, six independent $[Me_4N]^+$ cations and six MeCN molecules all located in general positions. Although the unit-cell parameters are very similar to those of $[Me_4N]_7[Ni_{42+y}C_8(CO)_{44+y}(CdCl)]\cdot(5–y)MeCN$ (y = 0.19), there is a significant volume difference between the two crystals (13331.3 vs. 12754 Å^3), in keeping with the substitution of one of the $[Me_4N]^+$ cations with a slightly smaller MeCN molecule. The Ni(43)C(12A)O(12A) group has a partial occupancy factor [0.190(4) after refinement]. To improve the model, the CO ligands bridging Ni(44) were also split. PART 1 of the model contains Ni(43), C(12A), O(12A), C(53), O(53), C(27A) and O(27A), whereas PART 2 contains C(12), O(12), C(27), O(27) and one non-coordinated MeCN molecule. Also another CO ligand was split into two positions [namely C(52)O(52) and C(52A)O(52A), respectively] and refined with an independent occupancy factor. All MeCN molecules were refined isotropically. Similar *U* restraints were applied to the C, O and N atoms. Rigid bond restraints were applied to the anion. Restrained bond lengths were applied to the CO ligands, the MeCN molecules and the $[Me_4N]^+$ cations.

Supporting Information (see footnote on the first page of this article): Electrochemical studies on $[HNi_{36}C_8(CO)_{36}(Cd_2Cl_3)]^{4-}$ in MeCN solution (Figure S1), spectroelectrochemical studies on $[HNi_{36}C_8(CO)_{36}(Cd_2Cl_3)]^{4-}$ in MeCN solution (Figure S2), $[HNi_{42+x}C_8(CO)_{44+x}(CdCl)]^{6-}$ in dmf solution (Figure S3) and $[H_2Ni_{22}(C_2)_4(CO)_{28}(CdBr)_2]^{2-}$ in dmf solution (Figure S4), progressive anodic reoxidation of $[Ni_{22}(C_2)_4(CO)_{28}(CdBr)_2]^{6-}$ to $[Ni_{22}(C_2)_4(CO)_{28}(CdBr)_2]^{4-}$ in dmf solution (Figure S5).

Acknowledgments

Financial support of the Ministero dell'Istruzione, dell'Università e della Ricerca (MIUR PRIN2006) and the University of Bologna (Project CLUSTERCAT: Metal clusters as precursors for nanostructured materials for catalysis) is gratefully acknowledged.

[1] a) D. L. Feldheim, C. A. J. Fos (Eds.), *Metal Nanoparticles: Synthesis, Characterisation and Applications*, Marcel Dekker, New York, **2002**; b) G. Schmid, L. F. F. Chi, *Adv. Mater.* **1998**, *10*, 515–526; c) A. C. Templeton, W. P. Wuelfing, R. W. Murray, *Acc. Chem. Res.* **2000**, *33*, 27–36; d) A. P. Alivisatos, Y. Yin, *Nature* **2005**, *437*, 664–670; e) C. Burda, X. Chen, R. Narayanan, M. A. El-Sayed, *Chem. Rev.* **2005**, *105*, 1025–1102.

[2] a) U. Simon in *Metal Clusters in Chemistry* (Eds.: P. Braunstein, L. A. Oro, P. R. Raithby), Wiley-VCH, Weinheim, **1999**, pp. 1342–1363; b) G. Schmid, Y.-P. Liu, *Nano Lett.* **2001**, *1*, 405–407; c) M. H. V. Werts, M. Lambert, J.-P. Bourgoin, M. Brust, *Nano Lett.* **2002**, *2*, 43–47.

[3] C. Femoni, F. Kaswalder, M. C. Iapalucci, G. Longoni, S. Zacchini, *Coord. Chem. Rev.* **2006**, *250*, 1580–1604.

[4] a) G. Longoni, C. Femoni, M. C. Iapalucci, P. Zanello in *Metal Clusters in Chemistry* (Eds.: P. Braunstein, L. A. Oro, P. R. Raithby), Wiley-VCH, Weinheim, **1999**, pp. 1137–1158; b) G. Longoni, M. C. Iapalucci in *Clusters and Colloids* (Ed.: G. Schmid), Wiley-VCH, Weinheim, **1994**, pp. 91–77.

[5] a) V. G. Albano, A. Ceriotti, P. Chini, G. Ciani, S. Martinengo, W. M. Anker, *J. Chem. Soc., Chem. Commun.* **1975**, 859–860; b) E. G. Mednikov, S. A. Ivanov, L. F. Dahl, *Angew. Chem. Int. Ed.* **2003**, *42*, 323–327; c) C. Femoni, M. C. Iapalucci, G. Longoni, P. H. Svensson, J. Wolowska, *Angew. Chem. Int. Ed.* **2000**, *39*, 1635–1637; d) J. M. Bemis, L. F. Dahl, *J. Am. Chem. Soc.* **1997**, *119*, 4545–4546; e) A. Ceriotti, N. Masciocchi, P. Macchi, G. Longoni, *Angew. Chem. Int. Ed.* **1999**, *38*, 3724–3727.

[6] a) J. D. Roth, G. J. Lewis, X. Jiang, L. F. Dahl, M. J. Weaver, *J. Phys. Chem.* **1992**, *96*, 7219–7225; b) A. Ceriotti, F. Demartin, G. Longoni, M. Manassero, M. Marchionna, G. Piva, M. Sansoni, *Angew. Chem. Int. Ed. Engl.* **1985**, *24*, 708–710; c) C. Femoni, M. C. Iapalucci, G. Longoni, P. H. Svensson, P. Zanello, F. Fabrizi de Biani, *Chem. Eur. J.* **2004**, *10*, 2318–2326; d) P. D. Mlynek, M. Kawano, M. Kozee, L. F. Dahl, *J. Cluster Sci.* **2001**, *12*, 313–338.

[7] a) B. F. G. Johnson, C. M. Martin in *Metal Clusters in Chemistry* (Eds.: P. Braunstein, L. A. Oro, P. R. Raithby), Wiley-VCH, Weinheim, **1999**, pp. 877–912; b) R. B. King, *New J. Chem.* **1988**, *12*, 493–499; c) J. F. Halet, D. G. Evans, D. M. P. Mingos, *J. Am. Chem. Soc.* **1988**, *110*, 87–90.

[8] a) T. Chihara, R. Komoto, K. Kobayashi, H. Yamazuki, Y. Matura, *Inorg. Chem.* **1989**, *28*, 964–967; b) P. J. Bailey, B. F. G. Johnson, J. Lewis, M. McPartlin, H. R. Powell, *J. Organomet. Chem.* **1989**, *377*, C17–C22.

[9] a) P. F. Jackson, B. F. G. Johnson, J. Lewis, M. McPartlin, W. J. H. Nelson, *J. Chem. Soc., Chem. Commun.* **1982**, 49–51; b) P. F. Jackson, B. F. G. Johnson, J. Lewis, M. McPartlin, W. J. H. Nelson, *J. Chem. Soc., Chem. Commun.* **1980**, 224–226; c) S. R. Drake, B. F. G. Johnson, J. Lewis, W. J. H. Nelson, M. D. Vargas, T. Adatia, D. Braga, K. Henrick, M. McPartlin, A. Sironi, *J. Chem. Soc., Dalton Trans.* **1989**, 1455–1464.

[10] a) A. F. Masters, J. T. Meyer, *Polyhedron* **1995**, *14*, 339–365; b) J. K. Battie, A. F. Masters, J. T. Meyer, *Polyhedron* **1995**, *14*, 829–868.

[11] a) A. Ceriotti, G. Piro, G. Longoni, M. Manassero, N. Masciocchi, M. Sansoni, *New J. Chem.* **1988**, *12*, 501–503; b) A. Ceriotti, G. Longoni, M. Manassero, M. Perego, M. Sansoni, *Inorg. Chem.* **1985**, *24*, 117–120; c) A. Ceriotti, A. Fait, G. Longoni, G. Piro, L. Resconi, F. Demartin, M. Manassero, N. Masciocchi, M. Sansoni, *J. Am. Chem. Soc.* **1986**, *108*, 5370–5371; d) F. Calderoni, F. Demartin, F. Fabrizi de Biani, C. Femoni, M. C. Iapalucci, G. Longoni, P. Zanello, *Eur. J. Inorg. Chem.* **1999**, 663–671; e) A. Ceriotti, A. Fait, G. Longoni, G. Piro, F. Demartin, M. Manassero, N. Masciocchi, M. Sansoni, *J. Am. Chem. Soc.* **1986**, *108*, 8091–8092.

[12] A. Bernardi, C. Femoni, M. C. Iapalucci, G. Longoni, F. Ranuzzi, S. Zacchini, P. Zanello, S. Fedi, *Chem. Eur. J.* **2008**, *14*, 1924–1934.

[13] A. Bernardi, C. Femoni, M. C. Iapalucci, G. Longoni, S. Zacchini, *Inorg. Chim. Acta* **2009**, *362*, 1239–1246.

[14] A. Bernardi, C. Femoni, M. C. Iapalucci, G. Longoni, S. Zacchini, *Dalton Trans.* **2009**, 4245–4251.

[15] C. Femoni, M. C. Iapalucci, G. Longoni, S. Zacchini, *Chem. Commun.* **2008**, 3157–3159.

[16] G. Longoni, A. Ceriotti, M. Marchionna, G. Piro in *Surface Organometallic Chemistry: Molecular Approaches to Surface Catalysis* (Eds.: J. M. Basset, B. C. Gates, J. P. Candy, A. Choplin, M. Leconte, F. Quignard, C. Santini), Kluwer, Dordrecht, **1988**, pp. 157–172.

[17] a) A. Ceriotti, G. Longoni, L. Resconi, M. Manassero, N. Masciocchi, M. Sansoni, *J. Chem. Soc., Chem. Commun.* **1985**, 181–182; b) A. Ceriotti, G. Piro, G. Longoni, M. Manassero, L. Resconi, N. Masciocchi, M. Sansoni, *J. Chem. Soc., Chem. Commun.* **1985**, 1402–1403.

[18] a) P. Hooker, B. Tan, K. Klabunde, S. Suib, *Chem. Mater.* **1991**, *3*, 947–952; b) A. F. Wells, *Structural Inorganic Chemistry*, Oxford Science Publications, Oxford, **1987**; c) *ASM Handbook*, Vol. 3 "Alloy Phase Diagrams" (Eds.: E. H. Kottcamp, E. L. Langer), ASM International, Ohio, **1992**, p. 2.112.

[19] P. Zanello, *Inorganic Electrochemistry – Theory, Practice and Application*, Royal Society of Chemistry, Cambridge, **2003**.
[20] a) A.-C. Dupuis, *Prog. Mater. Sci.* **2005**, *50*, 929–961; b) C. Ducati, I. Alexandrou, M. Chhowalla, J. Robertson, G. A. J. Amaratunga, *J. Appl. Phys.* **2004**, *95*, 6387–6391; c) H. Dai, A. G. Rinzler, P. Nikolaev, A. Thess, D. T. Colbert, R. E. Smalley, *Chem. Phys. Lett.* **1996**, *260*, 471–475; d) W. Wunderlich, *Diamond Relat. Mater.* **2007**, *16*, 369–376.
[21] E. Keller, *SCHAKAL99*, University of Freiburg, **1999**.
[22] F. Fabrizi de Biani, M. Corsini, P. Zanello, H. Yao, M. E. Bluhm, R. N. Grimes, *J. Am. Chem. Soc.* **2004**, *126*, 11360–11369.
[23] G. M. Sheldrick, *SADABS, Program for empirical absorption correction*, University of Göttingen, **1996**.
[24] G. M. Sheldrick, *SHELX97, Program for crystal structure determination*, University of Göttingen, **1997**.
Received: April 21, 2010
Published Online: August 24, 2010

